Supporting Information

Synthesis, crystal structures, anticancer activities and molecular docking studies of novel thiazolidinone Cu(II) and Fe(III) complexes targeting lysosomes: special emphasis on their binding to DNA/BSA

Jia Shao,[‡a] Qiang Zhang,[‡b] Jing Wei,[c] Zhiguang Yuchi,[c] Peng Cao,[d] Shao-Qing Li,[b] Shan Wang,[a] Jing-Yuan Xu,[e] Shuang Yang,[f] Yi Zhang,*[a] Jin-Xia Wei*[g] and Jin-Lei Tian*[b]

a. Department of Pharmacy, Tianjin First Central Hospital, Tianjin 300192, P. R. China.
b. College of Chemistry, Nankai University, Tianjin 300071, P. R. China.
c. Tianjin Key Laboratory for Modern Drug Delivery & High-Efficiency, Collaborative Innovation Center of Chemical Science and Engineering, School of Pharmaceutical Science and Technology, Tianjin University, Tianjin 300072, P. R. China.
d. Key Laboratory of Drug Targets and Drug Leads for Degenerative Diseases, Affiliated Hospital of Integrated Traditional Chinese and Western Medicine, Nanjing University of Chinese Medicine, Nanjing 210023, P. R. China.
e. School of Pharmacy, Tianjin Medical University, Tianjin 300070, P. R. China.
f. Medical College of Nankai University, Tianjin 300071, P. R.China.
g. School of Chinese Materia Medica, Tianjin University of Traditional Chinese Medicine, Tianjin 301617, Tianjin 300617, P. R. China.

‡These authors contributed equally to this work.
*Email: tiant@nankai.edu.cn; wing_zh1821@sina.com; weijinxia19871017@163.com.

Figure captions：

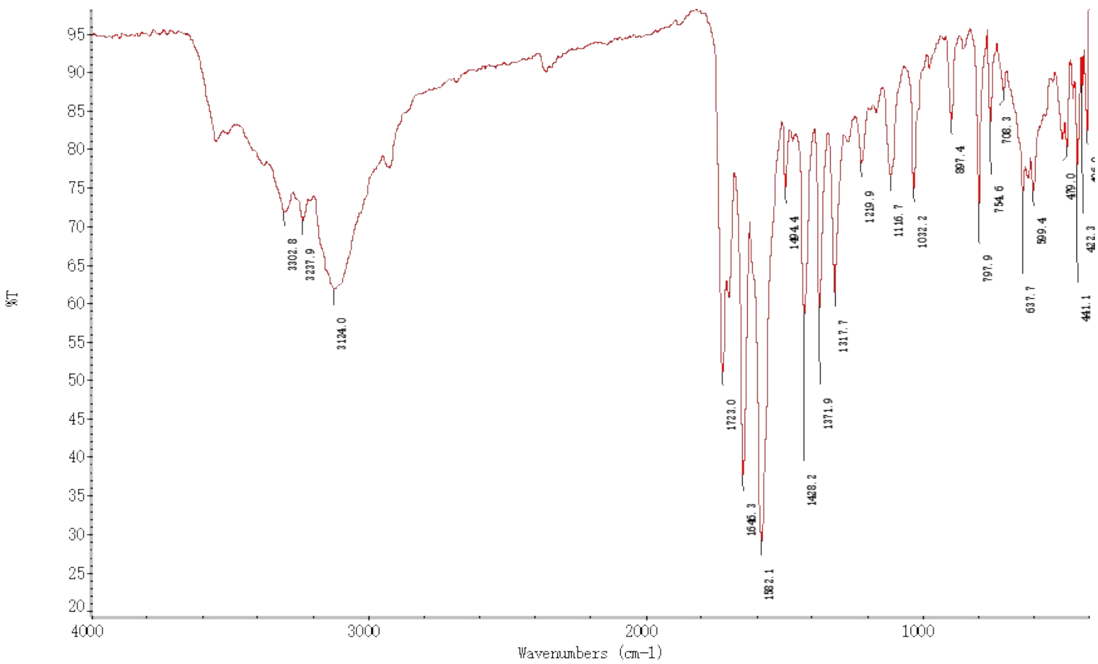

Figure S1 IR spectrum of $[Cu(\mathbf{L})_2Cl]\cdot Cl\cdot H_2O$ **(1)**.

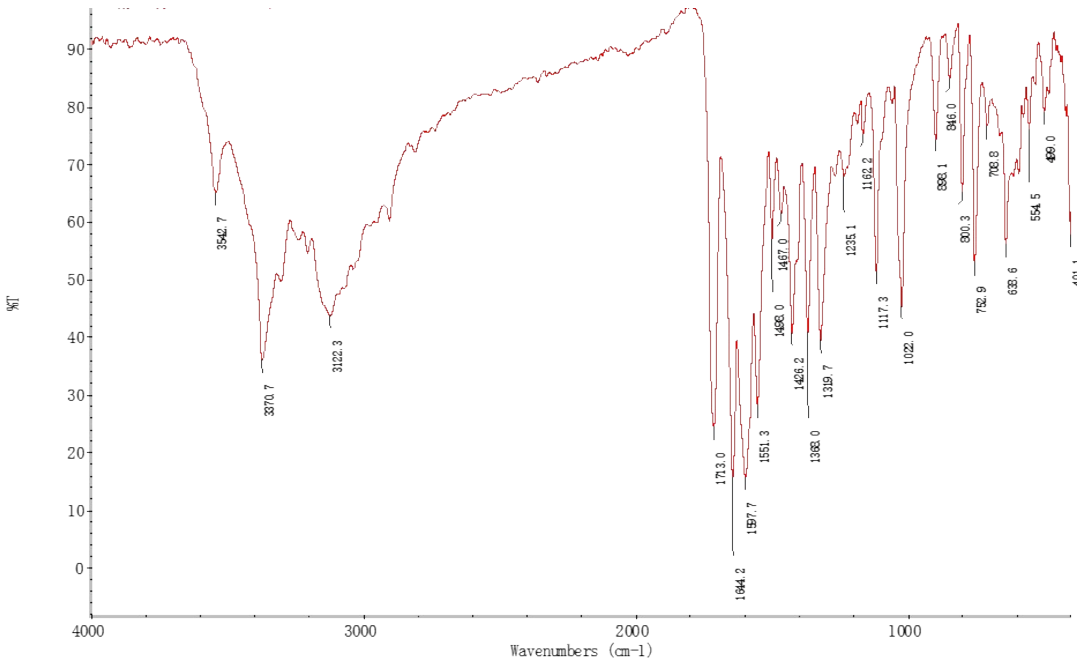

Figure S2 IR spectrum of $[Fe(\mathbf{L})_2Cl_2]\cdot Cl\cdot MeOH\cdot CHCl_3\cdot H_2O$ **(2)**.

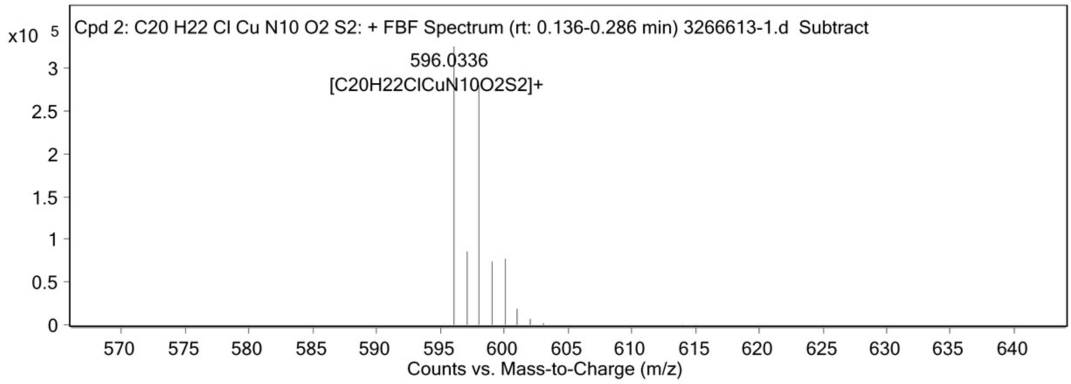

Figure S3 ESI-MS spectrum of $[Cu(\mathbf{L})_2Cl]\cdot Cl\cdot H_2O$ **(1)**.

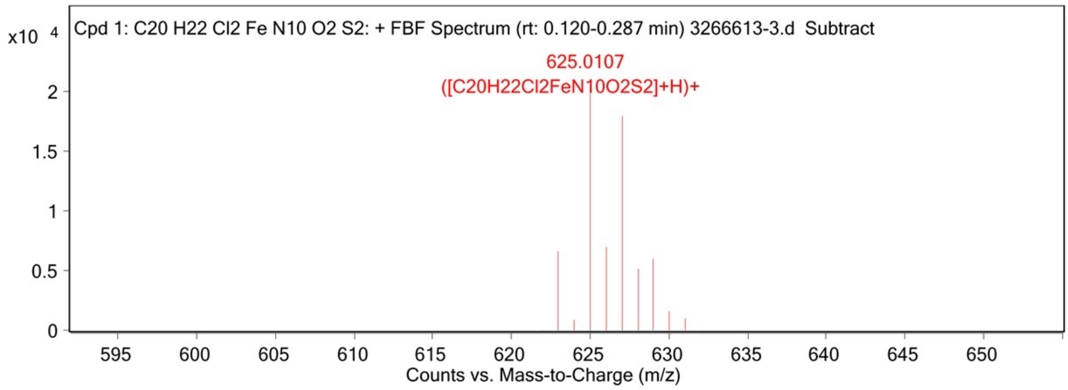

Figure S4 ESI-MS spectrum of $[Fe(\mathbf{L})_2Cl_2]\cdot Cl\cdot MeOH\cdot CHCl_3\cdot H_2O$ **(2)**.

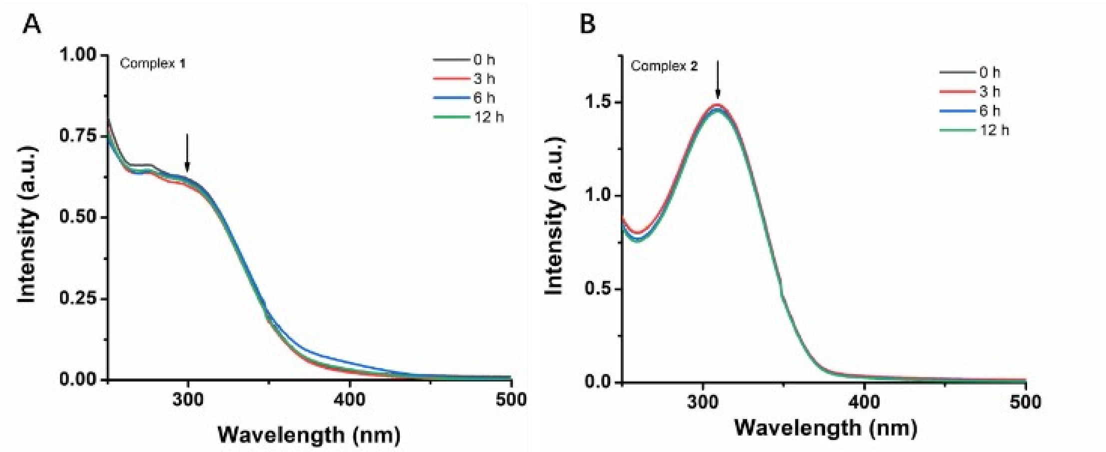

Figure S5 Absorption spectral traces of **1** (A) and **2** (B) in PBS at different times (0, 3, 6 and 12 h).

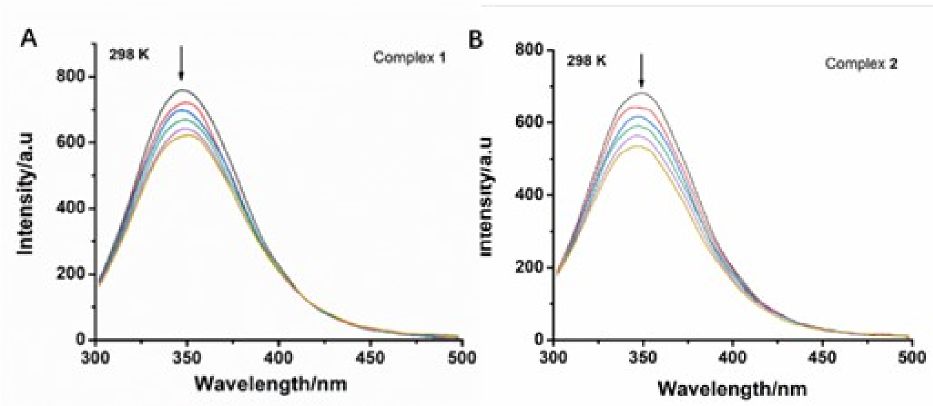

Figure S6 Fluorescence spectra of BSA in the different concentrations of **1** (A) and **2** (B) at 298 K. The concentrations of BSA (0.3 μM), complex **1** and **2** (0-0.97 μM).

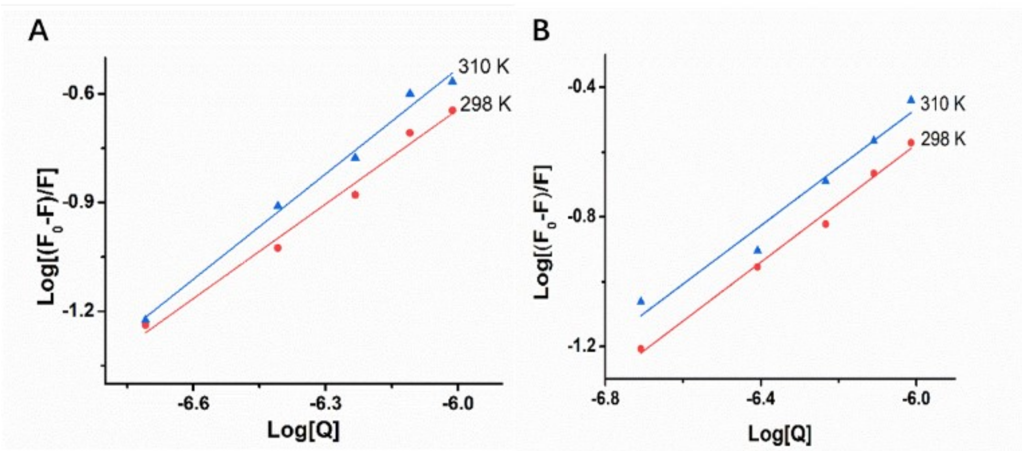

Figure S7 Plot of Log[(F_0 − F)/F] versus Log[Q].

Table S1 Comparison of DNA binding between analogues.

Compound	$K_{sv}\times10^3$ (M^{-1})	$K_b\times10^4$ (M^{-1})	$K_{app}\times10^5$(M^{-1})
Jia Shao (2021)			
$[Cu\mathbf{L}_2Cl]Cl\cdot H_2O$ (**1**)	5.98	8	2.40
$[Fe\mathbf{L}_2Cl_2]Cl\cdot MeOH\cdot CHCl_3\cdot H_2O$ (**2**)	16.2	11.5	6.49
Surbhi Jain (2020)[37]			
$[Cu(L1)(phen)](ClO_4)_2$	3.37	0.585	6.12
$[Cu(L1)_2](ClO_4)_2$	2.90	0.263	5.07
$[Cu(L1)(bipy)](ClO_4)_2\cdot H_2O$	2.54	0.101	4.38
$[Cu(L1)(imd)(ClO_4)](ClO_4)$	2.50	0.212	4.41
Nuno M. R. Martins (2017)[39]			
$[Cu(1_{\kappa}N,O^2{:}2_{\kappa}O\text{-}HL^1)(CH_3OH)]_2$	569 ± 20	27.2 ± 1.9	15.1
$[Cu(1_{\kappa}N,O^2{:}2_{\kappa}O\text{-}HL^1)((CH_3)_2NCHO)]_2$	596 ± 23	33.5 ± 2.1	16.0
$[Cu(_{\kappa}N\text{-}HL^1)\text{-}(en)_2]\ CH_3OH\cdot H_2O$	286 ± 12	17.2±3.2	8.9
$[Fe(_{\kappa}N^3\text{-}HL^2)_2]$	346 ± 13	19.8±2.6	9.5

Jessica Palmucci (2016)[40]			
$[Cu(H_2L^1)(H_2O)(im)]\cdot 3H_2O$	11.73 ± 0.12	0.176 ± 0.034	5.86
$[Cu(H_2L^3)(im)_2]\cdot H_2O$	5.42 ± 0.30	0.085 ± 0.021	2.71
Kang Zheng (2015)[41]			
$[Cu_2(chpoxd)(H_2O)(bpy)](NO_3)\cdot C_2H_5OH\cdot H_2O$	-	25.9 ± 8.8	8.33 ± 0.33
$[Cu_2(chmpoxd)\text{-}(H_2O)(bpy)]Cl\cdot 3H_2O$	-	13.8 ± 5.2	6.25 ± 0.23
Xue-Quan Zhou (2015)[42]			
$[Cu\mathbf{L2}^1Cl]ClO_4$	-	86.8	2.08
$[Cu\mathbf{L2}^1(acac)]PF_6$	-	49.7	2.15
$[Cu\mathbf{L2}^{2(R)}Cl]_2(PF_6)_2$	-	58.7	1.24
$[Cu\mathbf{L2}^{2(S)}Cl]_2(PF_6)_2$	-	173	1.26
$[Cu\mathbf{L2}^{2(R)}(acac)]PF_6$	-	115	2.09
$[Cu\mathbf{L2}^{2(S)}(acac)]PF_6$	-	346	2.18
Kang Zheng (2014)[38]			
$[Cu_2(pdmaeox)Cl(CH_3OH)(dabt)]\ CH_3OH$	95.9	8.35	-
$[Cu_2(pdmaeox)(bpy)(H_2O)]\text{-}(pic)\cdot H_2O$	56.9	3.39	-

Table S2 Comparison of BSA binding between analogues.

Compound	$K_{sv}\times10^5$ (M^{-1})	$K_q\times10^{13}$ (M^{-1}S^{-1})	$K_b\times10^5$ (M^{-1})	n
Jia Shao (2021)				
$[Cu\mathbf{L}_2Cl]Cl\cdot H_2O$ (**1**)	2.33	3.76	0.4	0.87
$[Fe\mathbf{L}_2Cl_2]Cl\cdot MeOH\cdot CHCl_3\cdot H_2O$ (**2**)	2.71	4.37	0.7	0.91
Surbhi Jain (2020)[37]				
$[Cu(L)(phen)](ClO_4)_2$	1.73	1.73	1.18	1.18 ± 0.07
$[Cu(L)_2](ClO_4)_2$	3.04	3.04	1.81	1.08 ± 0.07
$[Cu(L)(bipy)](ClO_4)_2\cdot H_2O$	2.30	2.30	1.40	1.135 ± 0.007
$[Cu(L)(imd)(ClO_4)](ClO_4)$	1.40	1.40	1.08	1.10 ± 0.008
Nuno M. R. Martins (2017)[39]				
$[Cu(1_{\kappa}N,O^2{:}2_{\kappa}O\text{-}HL^1)(CH_3OH)]_2$	11.6 ± 0.6	11.6	9.7±1	~1
$[Cu(1_{\kappa}N,O^2{:}2_{\kappa}O\text{-}HL^1)((CH_3)_2NCHO)]_2$	15.4 ± 0.7	15.4	11.9±0.9	~1
$[Cu(_{\kappa}N\text{-}HL^1)\text{-}(en)_2]\ CH_3OH\cdot H_2O$	2.2 ± 0.1	2.2	5.0 ± 0.1	~1
$[Fe(_{\kappa}N^3\text{-}HL^2)_2]$	6.0 ± 0.3	6.6	10.6 ± 0.8	~1
Jessica Palmucci (2016)[40]				
$[Cu(H_2L^1)(H_2O)(im)]\cdot 3H_2O$	1.048 ± 0.022	1.04 ± 0.02	-	-
$[Cu(H_2L^3)(im)_2]\cdot H_2O$	2.964 ± 0.085	2.96 ± 0.08	-	-
Kang Zheng (2015)[41]				
$[Cu_2(chpoxd)(H_2O)(bpy)](NO_3)\cdot C_2H_5OH\cdot H_2O$	-	-	-	-
$[Cu_2(chmpoxd)\text{-}(H_2O)(bpy)]Cl\cdot 3H_2O$	-	-	-	-
Xue-Quan Zhou (2015)[42]				
$[Cu\mathbf{Li}^1Cl]ClO_4$	0.119	-	0.208	1.0
$[Cu\mathbf{Li}^1(acac)]PF_6$	0.170	-	0.153	0.99
$[Cu\mathbf{Li}^{2(R)}Cl]_2(PF_6)_2$	0.125	-	0.203	1.10
$[Cu\mathbf{Li}^{2(S)}Cl]_2(PF_6)_2$	0.133	-	1.28	1.25

$[CuLi^{2(R)}(acac)]PF_6$	0.142	-	0.159	1.01
$[CuLi^{2(S)}(acac)]PF_6$	0.166	-	0.106	0.96
Kang Zheng (2014)[38]				
$[Cu_2(pdmaeox)Cl(CH_3OH)(dabt)]\ CH_3OH$	0.87	0.87	0.383	0.9659
$[Cu_2(pdmaeox)(bpy)(H_2O)]\text{-}(pic)\cdot H_2O$	1.18	1.18	0.523	0.9836

Table S3 IC_{50} values (μM) obtained with different cell lines for 48 h.

Complex	IC_{50} (μM)			
	HeLa	MCF-7	A549	BEAS-2B
1	24.5 ± 1.4	25.0 ± 2.2	46.2 ± 2.3	22.7 ± 0.5
2	> 100	63.6 ± 4.2	> 100	> 100
Cisplatin	4.3 ± 0.05	4.7 ± 0.5	14.8 ± 1.3	3.2 ± 0.01